Supporting Information

Enhancement in Xerostomia Patient Salivary Lubrication using a Mucoadhesive

*Hongping Wan[1], Arjan Vissink[2], Prashant K. Sharma[1]**

[1]University of Groningen and University Medical Center Groningen, Department of Biomedical Engineering, Antonius Deusinglaan 1, 9713 AV Groningen, The Netherlands.

[2]University of Groningen and University Medical Center Groningen, Department of Oral Maxillofacial Surgery, Hanzeplein 1, 9713 GZ, Groningen, The Netherlands.

*Corresponding author: p.k.sharma@umcg.nl

Materials and Methods

Chi-C synthesis and characterization

Catechol was conjugated to the amine moieties of chitosan by active agent EDC N-(3-dimethylaminopropyl-N-ethylcarbodiimide hydrochloride (Kim et al. 2013; Wang, Song, et al. 2017; Wang, Li, et al. 2017). Briefly, Chitosan (130 kDa, 3.25 mmol, Sigma Aldrich, CAS no. 9012-76-4) and hydrocaffeic acid (HCA, 3.25, 6.49, or 9.75 mmol, Sigma Aldrich, CAS no.1078-61-1) were dissolved in PBS (50mL pH=5). EDC (3.25, 6.49 or 9.75 mmol, Sigma Aldrich, CAS no. 25952-53-8) was then added to the mixture and stirred at room temperature for 12 hours. After extensively dialyzed (Mw cutoff: 3500, USA), the product was lyophilized and determined by ^{1}H-NMR (Bruker Avance, 400MHz, D_2O). The degree of catechol substitution determined by Uv-Vis spectrum at 280 nm with the standard hydrocaffeic acid curve with different concentrations ranging from 0.1mM to 0.9 mM in PBS by linear fitting. After obtaining the absorbance of 1 mg/ml Chi-C at 280nm the conjugate degree can be calculated.

Saliva collection and preparation

A standard protocol was followed to collect and prepare stimulated (SWS) and reconstituted (RWS) whole saliva(Veeregowda et al. 2013). SWS was collected from 4 healthy volunteers and 4 patients with primary Sjögren's syndrome. The patients with primary Sjögren's syndrome

fulfilled the 2016 ACR-EULAR classification criteria for Sjögren's syndrome (Shiboski et al. 2017). Participants did not eat and drink for one hour in advance. Before collecting any saliva, the mouth was rinsed well with water. Participant saliva was stimulated by chewing on parafilm to generate saliva for 15 minutes. The participants were instructed to expectorate saliva in pre weighed ice cooled flasks. After expectoration the flasks were weighed again and the volume of saliva estimated by using the saliva density of 1g/ml. Collected SWS was clarified by centrifugation at 10000 rpm at 10°C for 5 minutes. The protease inhibitor phenylmethylsulfonyl fluoride was added to stabilize the SWS at final concentration of 1 mM. Stimulated whole saliva was collected from 4 healthy volunteers with flow rate of 3.36, 1.76, 1.04, 1.02 ml/min. Stimulated whole saliva was also collected from 4 patients treated at the Maxillofacial surgery department of the University medical Center Groningen (UMCG) with reduced salivary flow rates of 0.48, 0.72, 0.45, 0.98ml/min (Thomson et al. 1999; van der Putten et al. 2011), respectively.

X-ray photoelectron spectroscopy

The elemental composition of the S-SCF surface was acquired from the X-ray photoelectron spectroscopy (XPS, S-Probe, surface science instruments, mountain view, CA, USA). Both low resolution for broad scans and high resolution for C_{1s} and O_{1s} peaks were made, where O_{1s} peak can be split into two components, the fraction of O_{1s} peak at 532.7eV (% $O_{532.7}$) from carboxyl groups was used to calculate the amount of oxygen-related in glycoprotein i.e. mucin amount ($\%O_{glyco}$)(Veeregowda et al. 2012).

$$\%O_{glyco}=\%O_{532.7} * \%O_{total} \quad (1)$$

Where $\%O_{total}$ is the total percentage of oxygen.

Colloidal probe atomic force microscopy

Friction force and surface topography of bare and S-SCF coated QCM crystal were measured using the colloidal probe AFM(Veeregowda et al. 2013) (Nanoscope IV Dimension tm 3100) equipped with a Dimension Hybrid XYZ SPM scanner head (Veeco, New York, USA). Rectangular, tipless cantilevers (length 300±5um, width 35±3um) were glued with a silica-particle (Bangs laboratories, Fishers, IN, USA) of 21.83 µm in diameter and calibrated for their torsional and normal stiffness by AFM Tune IT v2.5 software(Ducker et al. 1991; Pettersson et al. 2007). The deflection sensitivity (α) of the colloidal probe was recorded at constant compliance with bare crystal in buffer to calculate the normal force (F_n) applied using

$$F_n=\Delta V_n * \alpha * K_n \quad (2)$$

where ΔV_n is the voltage output from the AFM photodiode due to the normal deflection of the colloidal probe. The torsional stiffness and geometrical parameters of the probe were used to calculate the friction force (F_f)(Pettersson and Dedinaite 2008) according to

$$F_f=(\Delta V_L * K_t) / 2\delta * (d + t/2) \quad (3)$$

where t is the thickness of the cantilever, δ is the torsional detector sensitivity of the AFM and ΔV_L corresponds to the voltage output from the AFM photodiode due to lateral deflection of the probe. Lateral deflection was observed at a scanning angle of 90 degrees over a scan line of 10 µm and a scanning frequency of 1 Hz. The colloidal probe was incrementally loaded and unloaded up to a normal force (F_n) of 40 nN. At each normal force, friction loops were recorded to yield the average friction force, F_f.

Dental erosion and biocompatibility

Dental erosion was tested using an established protocol (Jager et al. 2008; Jager et al. 2012) . Bovine enamel was chosen here because the high homology of incisors samples between bovine and human (De Dios Teruel et al. 2015). In short, bovine incisors (8 × 6 mm) polished flat

(1200 grit grinding paper) and cleaned with deionized water, were partly covered with PVC tape exposing an area of approximately 5 × 3 mm in the center of the enamel. S-SCF with or without 0.5 mg/ml Chi-C treatment coated to the enamel surface (the same procedure as QCMD experiments), finally exposed to 50 mM citric acid in PBS for 30 min. The erosion depth then analyzed by optical coherence tomography (OCT Ganymade, Thorlabs Inc., Munich, Germany). For biocompatibility, a mouse fibroblastic cell line (L929) was acquired to co-cultured with S-SCF with Chi-C treatment and cell proliferation and metabolic activity measured by XTT(Zhou et al. 2017). Briefly, different S-SCF with or without Chi-C treatment were coated on the circular glass slide (15mm ϕ) surface that fit for the 24 cell culture plate. L929 with a concentration of 5×10^3 cells/well in a medium of high glucose DMEM (Gibco), 10% FBS (Gibco), and 1% penicillin-streptomycin (Sigma) were seeded on the surface for 1d, 3d and 7d culture. At each cultured period, XTT for metabolic activity by microplate reader recording absorbance at 485 and 690 nm and DAPI staining for nuclear visualization by confocal laser scanning microscopy (CLSM) were measured.

Evaluation of the antimicrobial activity of Chi-C

The antibacterial activity of Chi-C was assessed against *S. mutans* (UA159). *S. mutans* was grown on brain heart infusion (BHI) agar plates at 37 °C for 24 h. Next an overnight culture (BHI) prepared from a single colony was diluted 1:20 in 100ml BHI and incubated at 37 °C for 16 h. Bacteria were harvested by centrifugation at 5000g after washed twice in PBS (2.5 mM K_2HPO_4, 2.5 mM KH_2PO_4) supplemented with 3% v/v BHI to maintain bacterial viability in suspension. Then suspension was sonicated (3 × 10 s, 30 W) in an ice-water bath (Vibra Cell Model 375,Sonics and Materials Inc., Danbury, CT, USA). The bacterial concentration was calculated by a Bürker-Türk counting chamber. Bacterial cultures (10^6 mL^{-1} in BHI) were dispensed into each well of a 96-well microtiter plate with different Chi-C and Chi

concentrations, with a step factor dilution of 2 starting from 4mg mL^{-1}, and incubated at 37 °C for 24 h. Following incubation, the minimal inhibitory concentration (MIC) was taken as the lowest antibiotic concentration that did not create visible turbidity. Then, 10 μL of bacterial suspensions of each well showing no turbidity were plated on BHI agar plates and incubated at 37 °C for 24 h. The minimal bactericidal concentration (MBC) was taken as the lowest concentration at which no colonies were visible on the plate.

Time-kill kinetics. *S.mutans* (UA159) cultures (1×10^6 mL^{-1} in phosphate buffer supplemented with BHI) were diluted 1 : 10 in Chi-C and control Chi solutions in phosphate buffer. After 0, 1, and 2 h, suspensions were serially diluted in PBS (10 mM potassium phosphate) and 100 μL aliquots were plated on BHI agar plates and incubated for 24 h at 37 °C. The number of colonies formed on the plate was then manually counted.

Results:

Preparation and characterization of Chi-C

Figure S1 shows the synthesis and characterization of three conjugates of Chi-C with three equivalent proportions (1:1, 1:2, 1:3) between chitosan and hydrocaffeic acid (figure S1a). The conjugate were analyzed by H-NMR spectra and UV-Vis spectrometry as shown in Fig. S1b-c. The NMR spectra in Fig. 1b, where multiplets observed between δ = 6.5 ppm and δ = 7.0 ppm are associated with protons of the catechol(Kim et al. 2013; Kim et al. 2015); the region around 2 ppm corresponds to protons from acetyl, demonstrating the Chi-C conjugation was successful. The adsorption band at 280 nm of Uv-Vis spectrum in Fig. S1c, the characteristic band of the aromatic ring, confirms the conjugation successful. The conjugation degree was calculated using the standard curve of hydrocaffeic acid in Fig. S2. After obtaining the absorbance of 1 mg/ml Chi-C at 280 nm in Fig.S1c the conjugate degree was calculated as 7.6% (Chi-$C_{7.6\%}$), 14.5% (Chi-$C_{14.5\%}$) and 22.4% (Chi-$C_{22.4\%}$). These conjugations degrees cover the whole range

which is commonly used in literature (Kim et al. 2015; Wang, Li, et al. 2017), thus we used them to investigate their benefits on lubrication and dental erosion.

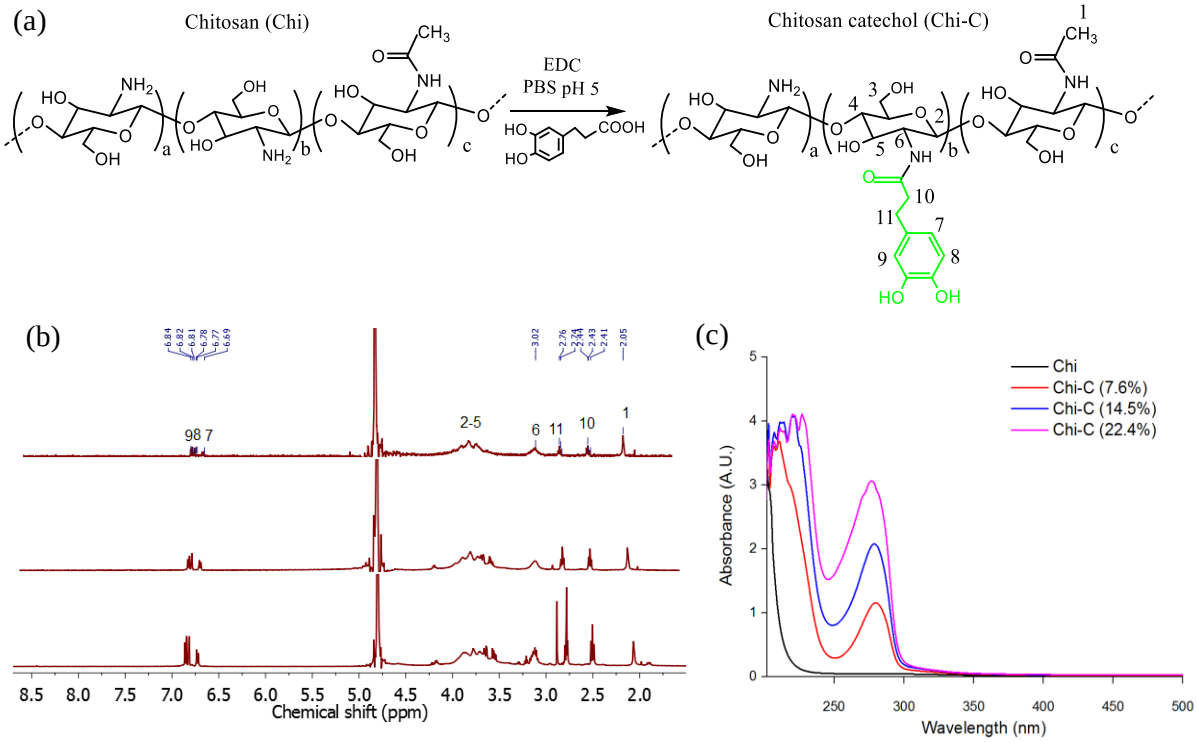

Figure S1. Chi-C synthesis and characterization. (a) is the synthesis route and the final structure of Chi-C. (b) and (c) are[1] H-NMR spectra and Uv-vis spectra of Chi-C respectively.

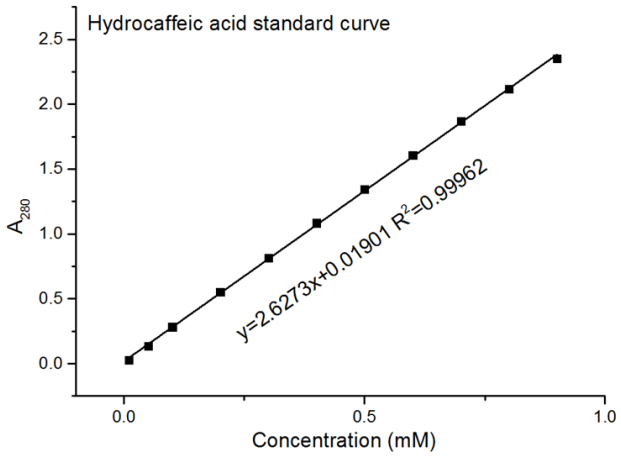

Figure S2. Uv-Vis spectra of hydrocaffeic acid solution at A_{280} with different concentration from 0.1mM to 0.9mM and the standard curve was calculated by linear fitting. Once we get the absorbance of 1 mg/ml Chi-C at 280 nm the conjugate degree can be calculated.

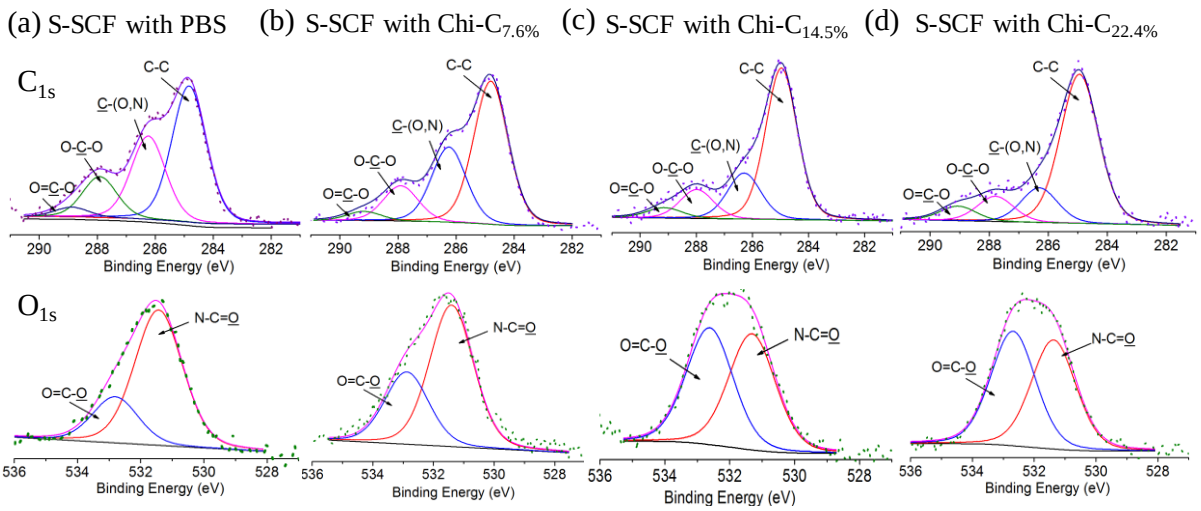

Figure S3 XPS analysis elemental composition of S-SCF treated with (a) buffer; (b) Chi-$C_{7.6\%}$; (c) Chi-$C_{14.5\%}$ and (d) Chi-$C_{22.4\%}$ and the decomposition of C_{1S} and O_{1S}. C_{1s} spectra of each surface could be deconvoluted into four different curves: C−(C,H), C−N/C−O, O−C−O, O−C=O and their percentages for S-SCF with PBS or S-SCF with various kind of Chi-C is different, suggesting different protein were detected from surface. As for the O_{1s} spectra, the relative contents of glycoprotein(Veeregowda et al. 2012) could be calculated by integral of O_{1s} at 532.7ev.

Table S1 Elemental composition of S-SCF treated with buffer, Chi-$C_{7.6\%}$, Chi-$C_{14.5\%}$, and Chi-$C_{22.4\%}$. ± indicates standard deviation over three measurements.

%	SCF with buffer		SCF with Chi-$C_{7.6\%}$	SCF with Chi-$C_{14.5\%}$	SCF with Chi-$C_{22.4\%}$
C	51.9±1.65		56.63±2.4	56.68±1.35	54.8±3.5
N	8.33±0.39		9.2±1.5	9.45±0.5	9.3±1.7
O	O_{total}	14.61±0.94	15.4±3.7	18.25±0.64	19.9±2.1
	$\%O_{532.7}*O_{total}$	5.39±2.25	7.04±2.6	9.35±1.3	9.88±1.6
K	8.72±3.8		7.01±2.8	5±0.56	8.5±1.4
Cl	7.87±3.7		6.08±1.49	5±0.99	7.8±0.35
P	8.95±0.92		4.64±0.19	5.2±1.37	3.45±1.2
Na	2.29±1.01		3.2±0.85	2.1±0.28	1.8±0.7

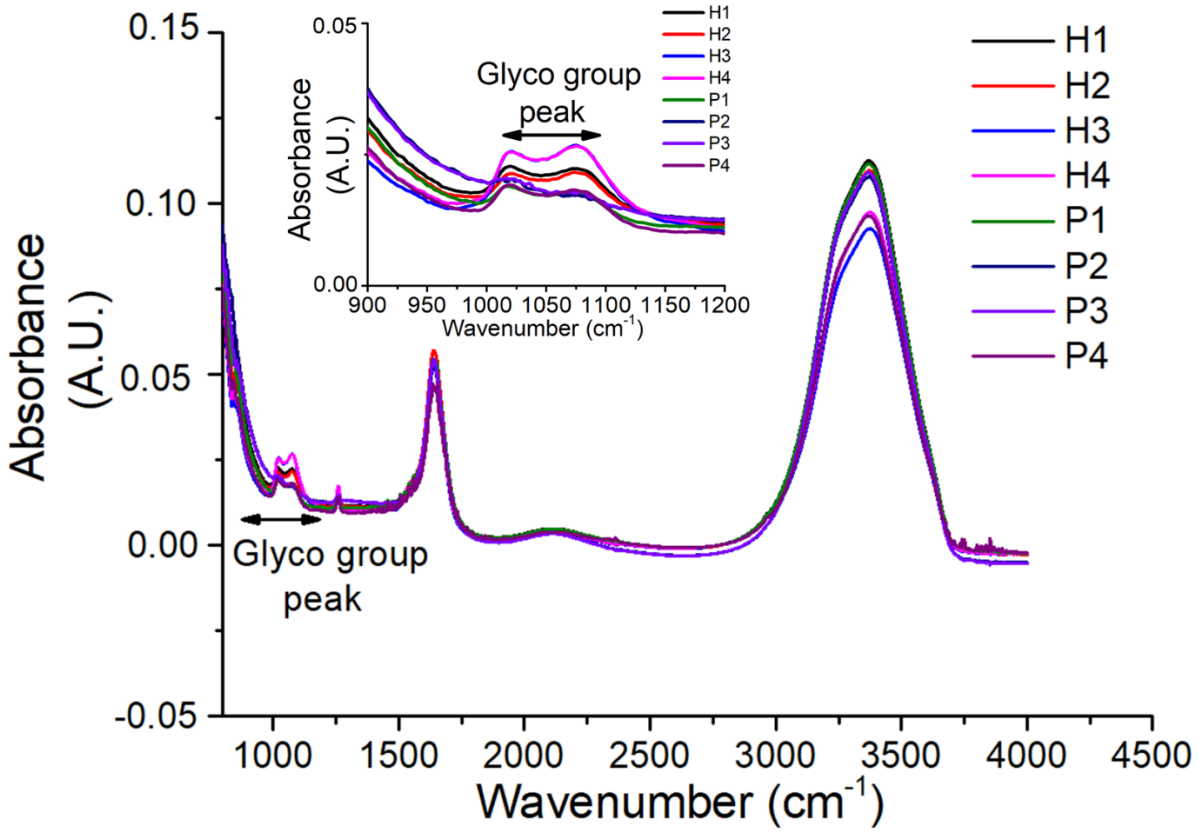

FigureS4. Typical FTIR adsorption bands for four patient saliva and healthy saliva measured in ATR-FTIR. 20 ul of each saliva (healthy saliva and patient saliva) was measured on a ATR-FTIR (Cary 600 series FTIR spectrometer, Agilent Technologies, Santa Clara, USA). Clearly visible glycol group peaks is from 950 to 1200 cm^{-1} and the absorbance band from 1600 and 1700 cm^{-1} related to the amide I peaks indicative of proteins. Water peaks belongs to area between 2500^{-1} cm and 4000 cm^{-1}. The higher absorbance and peak area of glycol group from all four healthy saliva were observed (zoomed in with the insertion) compared to the patient saliva, indicating less glycosylation of mucin in patient saliva

Table S2. MIC and MBC of Chi-C for oral bacterial *S. mutans(UA159)*

	MIC (mg/ml)	**MBC (mg/ml)**
Chitosan	1	2
Chi-$C_{7.6\%}$	0.5	1
Chi-$C_{14.5\%}$	0.5	1
Chi-$C_{22.4\%}$	0.5	1

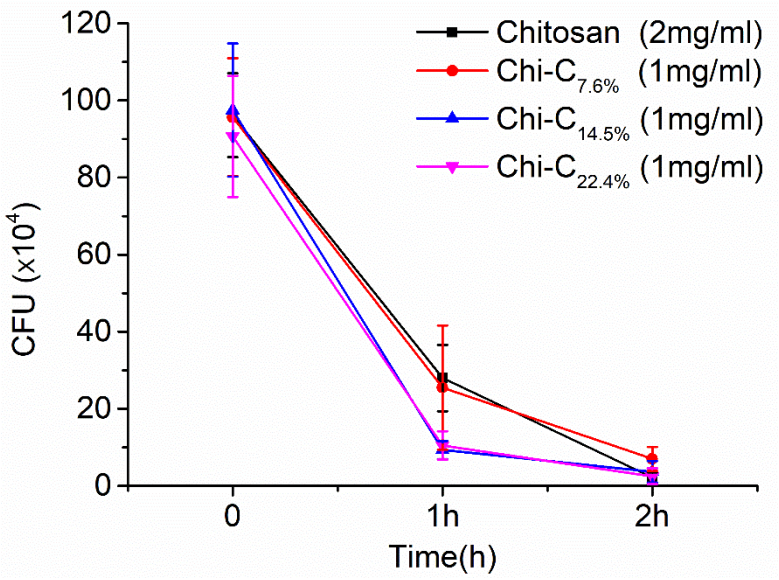

Figure S5. Efficacy of Chi-C kill *S. mutans*. Table S2 the MIC and MBC of Chitosan and Chi-C with various conjugation degree.

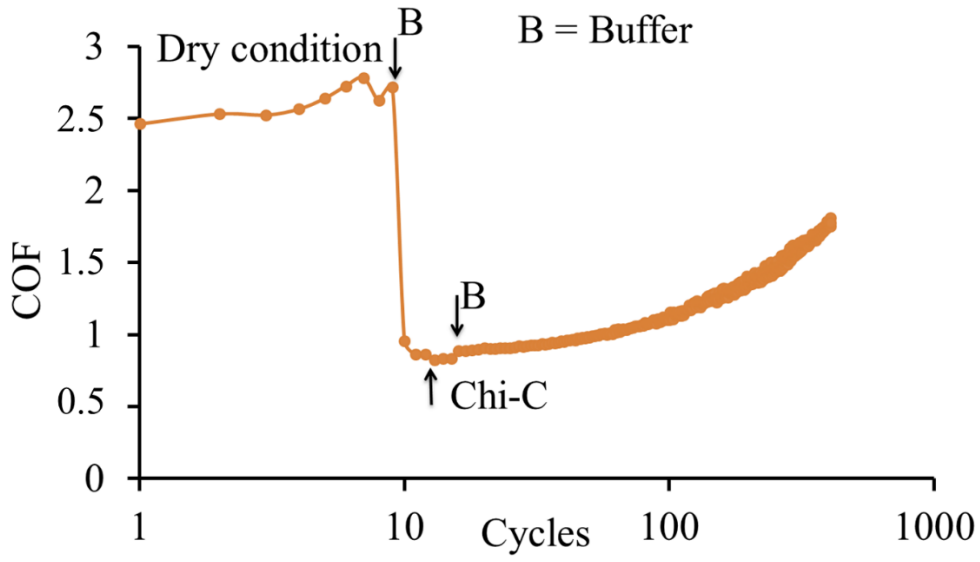

Figure S6. Lubrication property of Chi-C. To be consistent with HS and PS with or without Chi-$C_{22.4\%}$ treatment on tongue-enamel friction system. The lubrication property of Chi-$C_{22.4\%}$ was evaluated. The relief of Chi-$C_{22.4\%}$ is only 3.2 ± 1.4 folds lower than the HS (5.1 ±1.1) and PS (5.0 ± 1.3) and the relief period is even shorter only 2.5 ± 1.2 min indicating that Chi-C alone without reflow of saliva and formation of S-SCF is unable to provide a good lubrication.

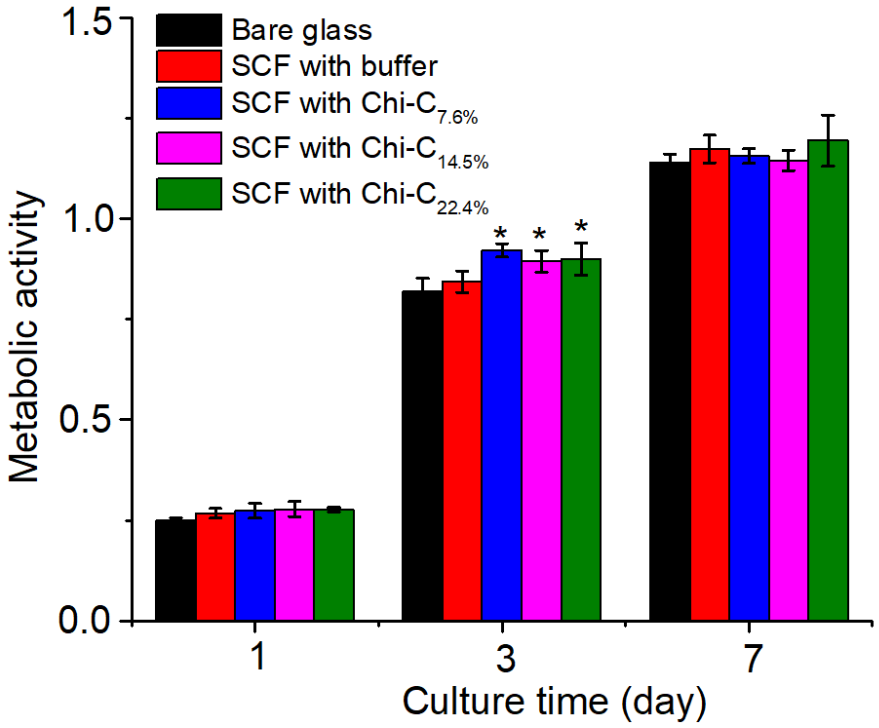

Figure S7. Human kidney epithelial cells were cocultured with different SCF after treatment by Chi-C and the metabolic activity measured by XTT. No significant different were detected on 1 and 7 cell culture day. On 3 day cells on SCF with Chi-$C_{14.5\%}$ and Chi-$C_{22.4\%}$ showed a higher metabolic activity compare to the bare glass. This result indicates no toxicity of Chi-C for epithelial cells. Statistical differences are marked with *, which stands for p-value < 0.05.

References:

Ducker WA, Senden TJ, Pashley RM. 1991. Direct measurement of colloidal forces using an atomic force microscope. Nature. 353(6341):239.

Jager DHJ, Vieira AM, Ruben JL, Huysmans MCDNJM. 2008. Influence of beverage composition on the results of erosive potential measurement by different measurement techniques. Caries Res. 42(2):98–104.

Jager DHJ, Vieira AM, Ruben JL, Huysmans MCDNJM. 2012. Estimated erosive potential depends on exposure time. J Dent. 40(12):1103–1108.

Kim K, Ryu JH, Lee DY, Lee H. 2013. Bio-inspired catechol conjugation converts water-insoluble chitosan into a highly water-soluble, adhesive chitosan derivative for hydrogels and LbL assembly. Biomater Sci. 1(7):783.

Kim Kyuri, Kim Keumyeon, Ryu JH, Lee H. 2015. Chitosan-catechol: A polymer with long-lasting mucoadhesive properties. Biomaterials. 52(1):161–170.

Pettersson T, Dedinaite A. 2008. Normal and friction forces between mucin and mucin-chitosan layers in absence and presence of SDS. J Colloid Interface Sci. 324(1–2):246–56.

Pettersson T, Nordgren N, Rutland MW, Feiler A. 2007. Comparison of different methods to calibrate torsional spring constant and photodetector for atomic force microscopy friction measurements in air and liquid. Rev Sci Instrum. 78(9):93702.

van der Putten GJ, Brand HS, Schols JMGA, de Baat C. 2011. The diagnostic suitability of a xerostomia questionnaire and the association between xerostomia, hyposalivation and medication use in a group of nursing home residents. Clin Oral Investig. 15(2):185–192.

Shiboski CH, Shiboski SC, Seror R, Criswell LA, Labetoulle M, Lietman TM, Rasmussen A, Scofield H, Vitali C, Bowman SJ, et al. 2017. 2016 American College of Rheumatology/European League Against Rheumatism Classification Criteria for Primary Sjögren's Syndrome: A Consensus and Data-Driven Methodology Involving Three International Patient Cohorts. Arthritis Rheumatol. 69(1):35–45.

Thomson WM, Williams SM, Thomsonr WM, Chalmers JM, Spencer AJ, Williams SM. 1999. The Xerostomia Inventory : A multi-item approach to measuring dry mouth The Xerostomia Inventorv : a multi-item approach to measuring dry mouth. 16(April):12–17.

Veeregowda DH, Busscher HJ, Vissink A, Jager DJ, Sharma PK, van der Mei HC. 2012. Role of structure and glycosylation of adsorbed protein films in biolubrication. PLoS One. 7(8).

Veeregowda DH, Kolbe A, Van Der Mei HC, Busscher HJ, Herrmann A, Sharma PK. 2013. Recombinant supercharged polypeptides restore and improve biolubrication. Adv Mater. 25(25):3426–3431.

Wang R, Li J, Chen W, Xu T, Yun S, Xu Zheng, Xu Zongqi, Sato T, Chi B, Xu H. 2017. A Biomimetic Mussel-Inspired ε-Poly-l-lysine Hydrogel with Robust Tissue-Anchor and Anti-Infection Capacity. Adv Funct Mater. 27(8).

Wang R, Song X, Xiang T, Liu Q, Su B, Zhao W, Zhao C. 2017. Mussel-inspired chitosan-polyurethane coatings for improving the antifouling and antibacterial properties of polyethersulfone membranes. Carbohydr Polym. 168:310–319.

Zhou Q, Castañeda Ocampo O, Guimarães CF, Kühn PT, Van Kooten TG, Van Rijn P. 2017. Screening Platform for Cell Contact Guidance Based on Inorganic Biomaterial Micro/nanotopographical Gradients. ACS Appl Mater Interfaces. 9(37):31433–31445.